Analyst

Cite this: *Analyst*, 2011, **136**, 4732

www.rsc.org/analyst

PAPER

Electrochemical DNA sensor by the assembly of graphene and DNA-conjugated gold nanoparticles with silver enhancement strategy†‡

Lei Lin, Yang Liu, Longhua Tang and Jinghong Li*

Received 16th July 2011, Accepted 22nd August 2011
DOI: 10.1039/c1an15610a

Sensitive and selective detection of DNA is in urgent need due to its important role in human bodies. Many disorders, such as Alzheimer's disease and various cancers, are closely related with DNA damage. In this work, a novel electrochemical DNA biosensor was constructed on a DNA-assembling graphene platform which provided a robust, simple and biocompatible platform with large surface area for DNA immobilization. The as-designed DNA sensor was fabricated by directly assembling captured ssDNA on a graphene-modified electrode through the π–π stacking interaction between graphene and ssDNA bases. Then, the target DNA sequence and oligonucleotide probes-labeled AuNPs were able to hybridize in a sandwich assay format, following the AuNPs-catalyzed silver deposition. The deposited silver was further detected by differential pulse voltammetry. Owing to the high DNA loading ability of graphene and the distinct signal amplification by AuNPs-catalyzed silver staining, the resulting biosensor exhibited a good analytical performance with a wide detection linear range from 200 pM to 500 nM, and a low detection limit of 72 pM. Additionally, the biosensor was proved to be able to discriminate the complementary sequence from the single-base mismatch sequence. The simple biosensor is promising in developing electronic, on-chip assays in clinical diagnosis, environmental control, and drug discovery.

Introduction

The accurate and rapid detection of DNA has received unrivalled attention in the field of biomolecular sensing owing to its important role in future genetic-disease diagnosis. Electrochemical DNA sensors offer great promise for DNA sensing due to their high sensitivity, selectivity, low cost and ease of miniaturization. A lot of efforts have been directed toward the development of electrochemical DNA sensors.[1–3] In addition to label-free methods,[4–6] strategies which make use of labels as gold nanoparticles,[7–9] enzymes,[10,11] ferrocene,[12,13] and metal complexes[14,15] to enhance the performance of the sensors have also gained much attention. In particular, nanomaterials (*e.g.* carbon nanotube, gold nanoparticles) have become a prevalent theme in this field ever since they have been applied to electrochemical DNA sensors. The introduction of nanomaterials has really improved the analytical performance of the sensors, because their notable properties, such as biocompatibility, high surface-to-volume ratio, and chemical stability are beneficial to DNA adsorption and signal amplification.[16]

In recent years, researches on graphene, a robust carbon nanomaterial,[17,18] have been invigorated due to its unique properties; for instance, the fascinating two-dimensional structure as well as the peculiar electronic properties.[19] Besides its excellent conductivity, the non-covalent interaction between graphene and biomolecules such as π–π stacking or hydrogen bonding makes graphene a promising candidate for assembling with various biomolecules[20–22] as well as the electrocatalytic and sensing applications. Meanwhile, the high specific surface area of graphene contributes to the high loading concentration of biomolecules on it. These unique properties can be further used to construct different sensing platforms with outstanding performance, which have been exemplified by the applications of graphene–DNA composites in DNA analysis,[23–26] non-DNA molecules detection,[27,28] intracellular molecular probing,[29] *etc*.[30,31] Those novel designations suggest that graphene can be used to construct a biocompatible electrochemical sensing interface for high-performance DNA biosensing applications based on the assembly between graphene and DNA molecules.

In this work, we report a simple and stable electrochemical DNA sensor for special DNA sequence detection (Scheme 1) on a DNA-assembling graphene (GR) platform. The DNA sensor

Department of Chemistry, Beijing Key Laboratory for Analytical Methods and Instrumentation, Key Laboratory of Bioorganic Phosphorus Chemistry and Chemical Biology, Tsinghua University, Beijing 100084, China. E-mail: jhli@mail.tsinghua.edu.cn

† This article is part of a web theme in *Analyst* and *Analytical Methods* on Future Electroanalytical Developments, highlighting important developments and novel applications. Also in this theme is work presented at the Eirelec 2011 meeting, dedicated to Professor Malcolm Smyth on the occasion of his 60th birthday.

‡ Electronic supplementary information (ESI) available. See DOI: 10.1039/c1an15610a

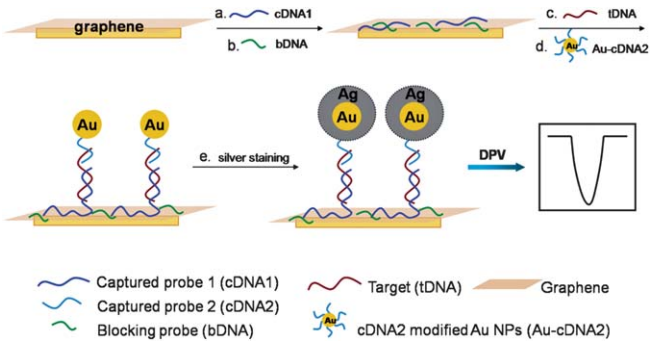

Scheme 1 Schematic diagram of the electrochemical DNA sensor. In a typical experiment, captured probe 1 (cDNA1) was adsorbed on the surface of a graphene-modified glassy carbon electrode directly (a), followed by a further adsorption of blocking probe (bDNA) (b). Different target sequences (c) and AuNPs-modified oligonucleotide probes (d) were then co-hybridized to the target-active substrates in buffer solution. After silver staining (e) on AuNPs tags as a signal amplification method, a subsequent DPV technique was applied as a detection means for deposited silver. The magnitude of the anodic peak current, which corresponds to the oxidation of silver particles, reflected the amount of complementary target oligonucleotides bound to the GCE-GR/cDNA1 surface.

was fabricated by the direct immobilization of captured DNA on the surface of a graphene-modified glassy carbon electrode (GCE) through the π–π stacking interaction between graphene and DNA. Gold nanoparticles (AuNPs)-modified oligonucleotide probes were then co-hybridized on the GCE surface in a sandwich assay format for the detection of targeted DNA sequence. In addition, a signal amplification based on silver staining on the AuNPs tags[32,33] was carried out and characterized by electrochemical stripping technique differential pulse voltammetry (DPV),[34–36] offering a distinct enhancement of the hybridization response. Comparing with conventional electrochemical DNA sensors, the as-designed DNA-assembling graphene platform has four superiorities on the construction of electrochemical DNA biosensor. First, the high specific surface area of graphene offered a high loading concentration of captured DNA on the electrode surface. Secondly, graphene provided a high electron transfer rate.[37,38] On the other hand, the strategy replaced the complicated procedures of conventional covalent DNA immobilization, and also avoided the electrochemical oxidation of the gold–sulfur bond during electrochemical measurements, providing a simple and stable electrochemical sensing platform. Additionally, the employment of the AuNPs-catalyzed signal amplification further enhanced the analytical performance of the biosensor. It is proved that this electrochemical DNA sensor was not only sensitive with a low detection limit, but was also capable of distinguishing a single-base mismatch sequence.

Experimental

1 Materials

Graphite (99.9%, 325 mesh) was purchased from Alfa Aesar. Tetrachloroauric(III) acid trihydrate ($HAuCl_4 \cdot 3H_2O$) was purchased from Sigma Aldrich Chemical Co. Other reagents were from Beijing Chemical Company. Buffers were prepared with deionized water. The DNA sequences and 10× TBE buffer were obtained from Shanghai Sangon Biological Engineering Technology & Services Co., Ltd. Sequences of oligonucleotide probes are listed as follows:

- Capture probe 1 (cDNA1): 5′-(GTG TGT)$_5$ GAG GAC ATT ATT AAT-3′;
- Capture probe 2 (cDNA2): 5′-AGA TGT CAA CAA TAT-C6-thiol-3′;
- Complementary target (tDNA): 5′-ATA TTG TTG ACA TCT ATT AAT AAT GTC CTC-3′;
- Non-complementary target: 5′-GAG GAC ATT ATT AAT AGA TGT CAA CAA TAT-3′;
- Single-base mismatch target: 5′-ATA TTG TCG ACA TCT ATT AAT AAT GTC CTC-3′;
- Blocking probe (bDNA): 5′-TTG AGA CTG GCA GTC GAA TTC-3′.

The synthesis of graphene, AuNPs and cDNA2-modified AuNPs (Au-cDNA2) is detailed in the Supporting Information.‡

2 Preparation of GCE-GR/cDNA1

1 mg graphene was dispersed in 1 mL DMF with ultrasonication for 1 h. 10 μL graphene–DMF solution was dropped onto a GCE and allowed to dry at room temperature to obtain the graphene-modified GCE (GCE-GR). Next, the GCE-GR was incubated in the 0.5× TBE buffer (pH 8.0) containing 2.3 μM cDNA1 at 4 °C for 6 h to yield the cDNA1-adsorbed GCE-GR (GCE-GR/cDNA1), followed by further incubation in 500 nM bDNA solution at 4 °C for another 6 h. The electrode surface was then gently rinsed with the washing buffer (0.5× TBE, 10 mM $NaNO_3$) for 5 min.

3 Hybridization reaction

The hybridization reaction was carried out by immersing the GCE-GR/cDNA1 in the target oligonucleotides-containing reaction buffer (0.5× TBE, 300 mM $NaNO_3$) at 35 °C for 1 h, which obtained the target DNA (tDNA) hybridized GCE-GR/cDNA1 (GCE-GR/cDNA1/tDNA). After careful rinsing with the washing buffer, the prepared electrode was immersed in 50 μL cDNA2-modified AuNPs (Au-cDNA2) solution at 35 °C for 1 h, yielding the Au-cDNA2 hybridized GCE-GR/cDNA1/tDNA (GCE-GR/cDNA1/tDNA/Au-cDNA2). Finally, the resulting electrode was rinsed with the washing buffer and dried under a stream of nitrogen.

4 Silver staining and electrochemical analysis

The resulting electrode was then incubated in fresh prepared silver enhancer solution (0.255 g citric acid, 0.24 g trisodium citrate, 0.01 g hydroquinone, 0.35 mg $AgNO_3$, 0.03 g sodium thiosulfate pentahydrate and 10 mL deionized water)[39] for 10 min in the dark, followed by full washing with double-distilled water. DPV detection of the deposited Ag was carried out in 0.1 M KNO_3 (pH 7.0) with a positive scan from −0.1 V to 0.3 V (*vs.* Ag/AgCl saturated with KCl).

5 Instruments

Transmission electron microscopy (TEM) images were collected using a Hitachi H-7650 TEM opened at an accelerating voltage of 80 kV. The UV-vis absorption spectra were obtained *via* a Hitachi U-3900 UV/Vis spectrophotometer. XRD patterns were obtained using a D8 Advance (Bruker) X-ray diffractometer using Cu-Kα radiation (λ = 1.5418 Å). Raman spectra were collected on a RM 2000 Microscopic confocal Raman spectrometer (Renishaw PLC, England) with a 633 nm He-Ne laser beam. Scanning electron microscopy (SEM) images were obtained using a LEO1530 field emission SEM system (Germany).

Electrochemical measurements were performed *via* DPV with a CHI-830 electrochemical analyzer (CHI Inc.) and electrochemical impedance spectroscopy (EIS) with a PARSTAT 2273 electrochemical system (Princeton Applied Research). The EIS was tested in 5 mM $K_3[Fe(CN)_6]/K_4[Fe(CN)_6]$ (1 : 1) aqueous solution with frequency from 0.1 Hz to 100 kHz and signal amplitude of 10 mV. Each electrochemical experiment was carried out in one conventional three-electrode system, which was comprised of a platinum counter electrode, a KCl saturated Ag/AgCl reference electrode and a modified GCE as the working electrode. Before use, the GCE was carefully polished with 0.3 and 0.05 μm Al_2O_3 powder successively and then rinsed with water, ethanol, acetone, water respectively, before being dried finally in nitrogen.

Results and discussion

1 The assembly of graphene and DNA-modified AuNPs on the electrode

To verify the assembly of the DNA sensing platform, cyclic voltammetry (CV) and electrochemical impedance spectroscopy (EIS) were used to characterize the GCEs modified step by step. The bare GCE (Fig. 1A, curve a) shows a couple of quasi-reversible redox peaks of the $Fe(CN)_6^{4-/3-}$ probes. After modification of the GCE with graphene, an obvious increase of the peak currents was observed (Fig. 1A, curve b). The fact is attributed to the large surface area and superior electronic transfer ability of graphene which not only greatly enhanced the electroactive sites but also accelerated the charge transfer at the electrode interface. The peak current decreased (Fig. 1A, curve c) after the assembly of cDNA1 and the following hybridization with tDNA due to the inert feature of DNA. When Au-cDNA2 were introduced, the peak current (Fig. 1A, curve d) increased slightly, which would be attributed to the good conductivity and the catalytic ability of the gold nanoparticles.

Electrochemical impedance spectra measure the impedance of a system over a range of frequencies. This technique provides a useful experimental method for characterizing electrochemical systems. Data from EIS are usually expressed graphically in a Nyquist plot. The diameter of the semi-circle at higher frequency range in the Nyquist plot represents the electron transfer resistance at the electrode interface, and it decreased after the modification of graphene on the GCE (Fig. 1B, curve b). The distinct increase of electron transfer resistance after the adsorption of cDNA1 and the following hybridization with tDNA confirmed their immobilization onto the GCE-GR surface. After the addition of Au-cDNA2, a decrease of electron transfer resistance was found, indicating the formation of the target DNA–AuNPs hybrid. These results were similar to those of the cyclic voltammograms. It is noted that the electron transfer resistance on the GCE-GR/cDNA1/tDNA was larger than that of the graphene-modified GCE, while a larger peak current was obtained on the GCE-GR/cDNA1/tDNA. The fact can be ascribed to the high specific surface area of graphene which provided many more electroactive sites. This unique property means that graphene is a promising platform in developing highly sensitive biosensors.

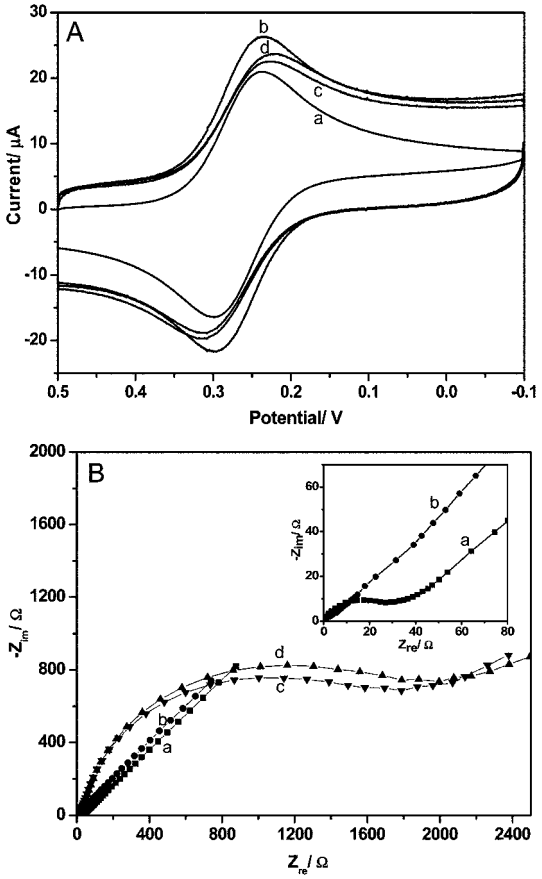

Fig. 1 Cyclic voltammograms (A) and Nyquist plot (B) of bare GCE (a), GCE-GR (b), GCE-GR/cDNA1/tDNA (c), GCE-GR/cDNA1/tDNA/Au-cDNA2 (d). Insert in (B): magnified Nyquist plot for bare GCE (a) and GCE-GR (b). Electrolyte: 5 mM $K_3[Fe(CN)_6]/K_4[Fe(CN)_6]$ (1 : 1) aqueous solution with 100 mM KCl. Frequency: from 0.1 Hz to 100 kHz. Amplitude: 10 mV. Scan rate: 100 mV s^{-1}.

Fig. 2A demonstrates the TEM image of graphene sheets. It clearly displays the flake-like shapes of graphene with ripples and edges. After hybridization with Au-cDNA2, as it illustrated in Fig. 2B, the graphene surface was decorated with AuNPs with an average diameter of 13 nm. SEM images in Fig. S3‡ show the surface topography of graphene and Au-cDNA2 hybridized graphene on the glassy carbon, respectively. It can be found that the graphene film exhibits uniform morphology over large areas with numerous wrinkles on the surface, which greatly increases the surface area of the GCE. The initial silver nucleation on AuNPs resulted in a successive precipitation of silver on

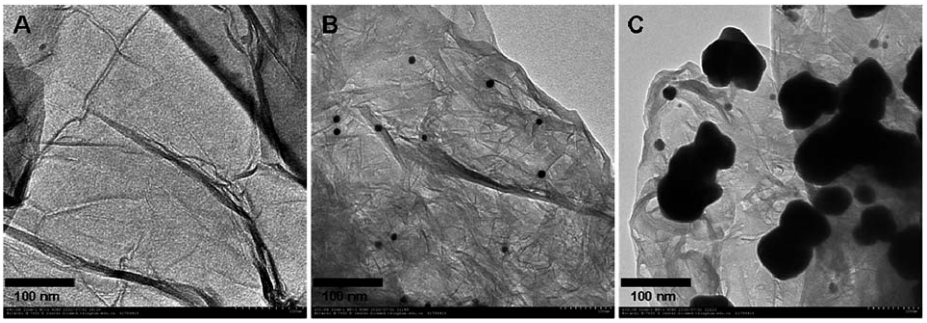

Fig. 2 TEM images of graphene (A), Au-cDNA2 hybridized graphene (B), and Au-cDNA2 hybridized graphene after silver staining (C).

nanoparticles and ultimately large silver particles formed. It is observed from Fig. 2C that the particle size was greatly increased after treatment in a stain. The obvious change in particle size means that silver deposition is successfully performed on the graphene surface.

2 Optimization of silver deposition time

Fig. 3 describes the effect of the silver staining time on the blank and the hybridization (200 nM complementary target) by DPV measurements. As shown, the peak currents increased when the deposition time was varied from 5 to 15 min. After 10 min, the DPV signal of the hybridization was approximately 17 times larger than that of the blank, yielding a maximum of the peak current ratio of the target hybridization to the blank (i_{target}/i_{blank}). Thus, the optimal reaction time for silver deposition was chosen to be 10 min. It has been reported that silver particles could grow through polyanionic DNA chains, because the cation Ag^+ tends to exchange with Na^+ and forms the ion-pair complex to the bases.[40] Therefore, an excess of silver staining time would make the DPV responses unreliable and bring on an enlargement of the background current. Furthermore, $Na_2S_2O_3$ fixer solution was used to eliminate the background current. In order to reduce the non-specific adsorption between Au-cDNA2 and graphene, the adsorption of blocking probe was further carried out. The obviously distinguished current intensity between the blank and target sample implies that the method can be applied to construct highly sensitive electrochemical DNA sensors.

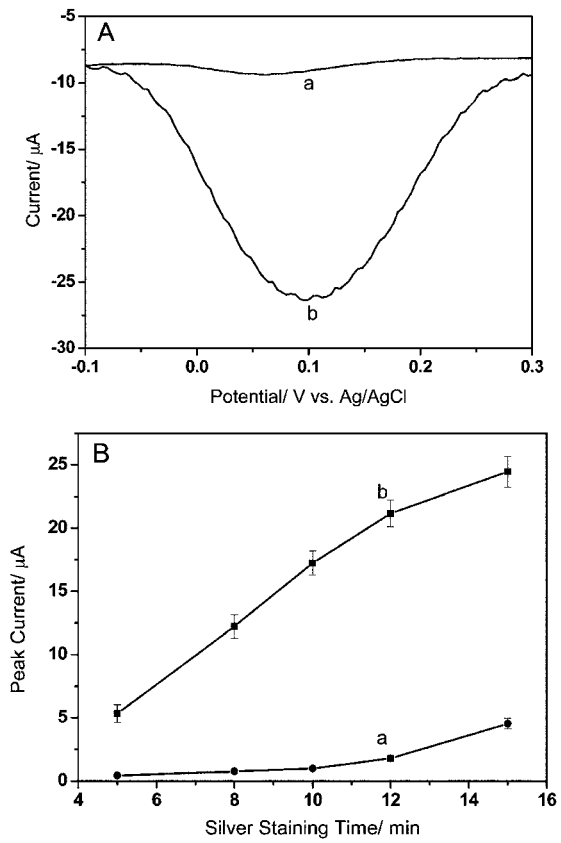

Fig. 3 (A) DPV response curves of the electrochemical DNA sensor in the blank (a) and 200 nM complementary target DNA (b) with 10 min as the silver staining time. (B) Effect of silver staining time on the silver response of blank (a) and 200 nM complementary target (b). Electrolyte: 0.1 M KNO_3. Pulse amplitude: 50 mV. Pulse period: 0.2 s.

3 Target detection of the electrochemical DNA biosensor

Owing to its higher sensitivity, DPV is widely used in the electrochemical sensing application for the detection of redox probes with low concentrations. Fig. 4A shows the DPV responses for different target DNA concentrations. Obviously, the peak currents gradually increased along with the target DNA concentration increases from 200 pM to 500 nM. The DPV signals were clearly amplified when the silver enhancement strategy was brought in. The amount of complementary target oligonucleotides bound to the GCE-GR/cDNA1 surface was reflected by the magnitude of the anodic peak current, which corresponds to the oxidation of silver particles. It is also seen that the oxidation peak potential of Ag shifted toward more positive values as the target DNA concentration was increased. This phenomenon may be ascribed to the increase in the thickness of the metallic film on an inert electrode, which causes the anodic peak to shift more positively.[41,42] The positive shift of peak potential dependent on the increase of the target DNA concentration is attributed to an increase in the thickness of the metallic film on an inert electrode, which caused the oxidation peak potential to shift toward more positive values.

Moreover, the peak current of the sensor was linearly increased with the logarithm of the target DNA concentration in range from 200 pM to 500 nM as shown in Fig. 4B. The linear relationship can be described as $I = 6.612 + 4.759\log c$ with the correlation coefficient of $R = 0.998$, where I is the peak current

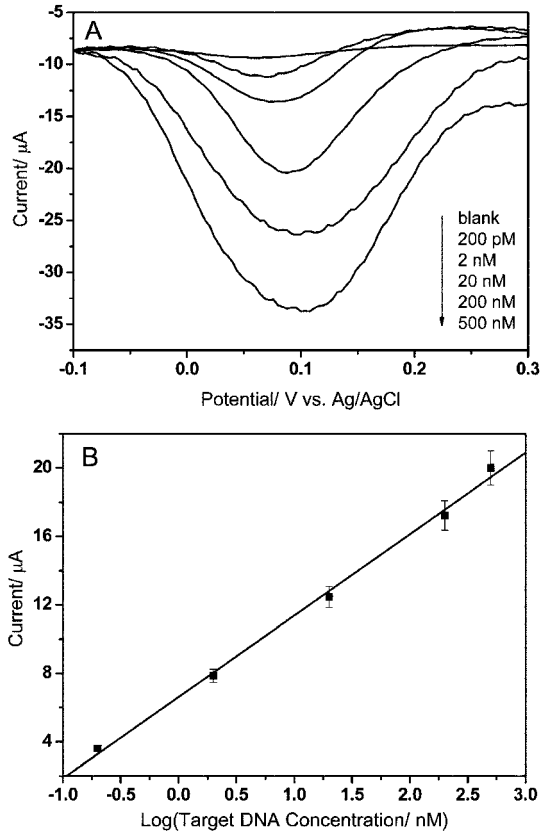

Fig. 4 (A) DPV response curves of the electrochemical DNA sensor at various complementary target DNA concentrations (top to bottom: 0, 0.2, 2, 20, 200, 500 nM) in 0.1 M KNO_3. Pulse amplitude: 50 mV. Pulse period: 0.2 s. (B) Linear relationship between the peak current and the logarithm of the target DNA concentration. Silver staining time: 10 min.

and log *c* is the logarithm of the target DNA concentration. The detection limit of target DNA was 72 pM (S/N = 3). This result suggests that the simple electrochemical DNA sensor can be applied to the sensitive DNA analysis over a wide concentration range.

4 Selectivity of the electrochemical DNA biosensor

To study the selectivity of the biosensor, three different DNA sequences were characterized based on the as-designed DNA biosensor. The concentration of the above sequences was 200 nM in each experiment. DPV responses were obtained after successive hybridization with Au-cDNA2 followed by silver staining. Fig. 5 shows the peak currents of the above-mentioned three target DNA sequences and blank solution. The complementary sequence exhibited the highest peak current (17.23 μA) among the blank (0.967 μA), non-complementary target (0.733 μA) and the single-base mismatch target (5.551 μA). It was obvious that peak current from the target DNA was much larger than that of other oligonucleotide sequences. The facts mean that the biosensor could be used to discriminate the complementary target from the single-base mismatch and the non-complementary sequences with high sensitivity and specificity.

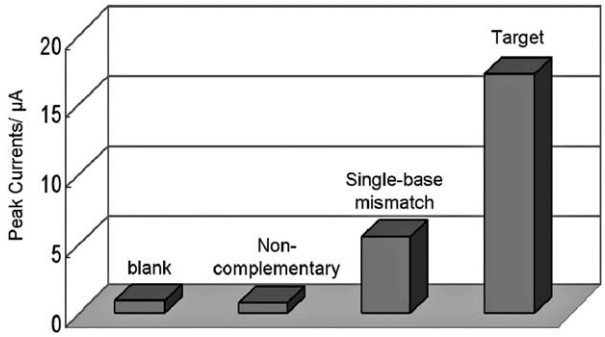

Fig. 5 DPV responses of the electrochemical DNA sensor in the blank, non-complementary sequence, single-base mismatch sequence and complementary sequence. Electrolyte: 0.1 M KNO_3. Pulse amplitude: 50 mV. Pulse period: 0.2 s. Silver staining time: 10 min.

Conclusion

In summary, a simple graphene sensing platform based on the π–π stacking interaction between graphene and ssDNA sequence was constructed, and a sensitive and selective electrochemical DNA sensor was fabricated for special DNA sequence analysis based on the sandwich assembly between graphene, target DNA and DNA-conjugated gold nanoparticles. The following silver staining on the gold nanoparticle improved the performances of the electrochemical DNA sensor. The as-prepared biosensor had a wide detection linear range as well as a low detection limit. Furthermore, it was capable of discriminating single-base mismatch sequences. As a result, the electrochemical DNA sensor should be promising in a diverse applications such as clinical diagnostics, food analysis and drug screening, *etc*.

Acknowledgements

This work was financially supported by National Basic Research Program of China (No. 2007CB310500, No. 2011CB935700), Tsinghua University Initiative Scientific Research Program and the Funding from State Key Laboratory of Chemo/Biosensing and Chemometrics, Hunan University, China.

References

1 A. A. Lubin and K. W. Plaxco, *Acc. Chem. Res.*, 2010, **43**, 496.
2 F. Lucarelli, S. Tombelli, M. Minunni, G. Marrazza and M. Mascini, *Anal. Chim. Acta*, 2008, **609**, 139.
3 B. J. Privett, J. H. Shin and M. H. Schoenfisch, *Anal. Chem.*, 2010, **82**, 4723.
4 S. Shrestha, C. Yeung, C. Mills, J. Lewington and S. Tsang, *Angew. Chem., Int. Ed.*, 2007, **46**, 3855.
5 F. Uslu, S. Ingebrandt, D. Mayer, S. Böcker-Meffert, M. Odenthal and A. Offenhäusser, *Biosens. Bioelectron.*, 2004, **19**, 1723.
6 Y. Jin, X. Yao, Q. Liu and J. H. Li, *Biosens. Bioelectron.*, 2007, **22**, 1126.
7 K. Hu, D. Lan, X. Li and S. Zhang, *Anal. Chem.*, 2008, **80**, 9124.
8 K. Kerman, Y. Morita, Y. Takamura, M. Ozsoz and E. Tamiya, *Anal. Chim. Acta*, 2004, **510**, 169.
9 Z. P. Wang, J. Q. Hu, Y. Jin, X. Yao and J. H. Li, *Clin. Chem.*, 2006, **52**, 1958.
10 J. Wang, G. Liu and M. R. Jan, *J. Am. Chem. Soc.*, 2004, **126**, 3010.
11 E. Williams, M. I. Pividori, A. Merkoçi, R. J. Forster and S. Alegret, *Biosens. Bioelectron.*, 2003, **19**, 165.
12 K. Kim, H. Yang, S. H. Park, D. S. Lee, S. J. Kim, Y. T. Lim and Y. T. Kim, *Chem. Commun.*, 2004, (13), 1466.

13 Y. Zhang, Y. Wang, H. Wang, J. H. Jiang, G. L. Shen, R. Q. Yu and J. H. Li, *Anal. Chem.*, 2009, **81**, 1982.
14 A. de la Escosura-Muniz, M. B. Gonzalez-Garcıa and A. Costa-Garcıa, *Biosens. Bioelectron.*, 2007, **22**, 1048.
15 D. Hernandez-Santos, M. B. Gonzalez-Garcıa and A. Costa-Garcıa, *Anal. Chem.*, 2005, **77**, 2868.
16 J. Wang, D. Xu, A. N. Kawde and R. Polsky, *Anal. Chem.*, 2001, **73**, 5576.
17 A. K. Geim and K. S. Novoselov, *Nat. Mater.*, 2007, **6**, 183.
18 K. S. Novoselov, A. K. Geim, S. V. Morozov, D. Jiang, Y. Zhang, S. V. Dubonos, I. V. Grigorieva and A. A. Firsov, *Science*, 2004, **306**, 666.
19 M. J. Allen, V. C. Tung and R. B. Kaner, *Chem. Rev.*, 2009, **110**, 132.
20 F. Liu, J. Y. Choi and T. S. Seo, *Chem. Commun.*, 2010, **46**, 2844.
21 A. J. Patil, J. L. Vickery, T. B. Scott and S. Mann, *Adv. Mater.*, 2009, **21**, 3159.
22 N. Varghese, U. Mogera, A. Govindaraj, A. Das, P. K. Maiti, A. K. Sood and C. N. R. Rao, *ChemPhysChem*, 2009, **10**, 206.
23 X. Dong, Y. Shi, W. Huang, P. Chen and L. J. Li, *Adv. Mater.*, 2010, **22**, 1649.
24 S. He, B. Song, D. Li, C. Zhu, W. Qi, Y. Wen, L. Wang, S. Song, H. Fang and C. Fan, *Adv. Funct. Mater.*, 2010, **20**, 453.
25 F. Liu, J. Y. Choi and T. S. Seo, *Biosens. Bioelectron.*, 2010, **25**, 2361.
26 C. H. Lu, H. H. Yang, C. L. Zhu, X. Chen and G. N. Chen, *Angew. Chem., Int. Ed.*, 2009, **48**, 4785.
27 H. Chang, L. Tang, Y. Wang, J. Jiang and J. H. Li, *Anal. Chem.*, 2010, **82**, 2341.
28 H. Dong, W. Gao, F. Yan, H. Ji and H. Ju, *Anal. Chem.*, 2010, **82**, 5511.
29 Y. Wang, Z. Li, D. Hu, C. T. Lin, J. H. Li and Y. Lin, *J. Am. Chem. Soc.*, 2010, **132**, 9274.
30 N. Mohanty and V. Berry, *Nano Lett.*, 2008, **8**, 4469.
31 Y. Wen, F. Xing, S. He, S. Song, L. Wang, Y. Long, D. Li and C. Fan, *Chem. Commun.*, 2010, **46**, 2596.
32 S. J. Park, T. A. Taton and C. A. Mirkin, *Science*, 2002, **295**, 1503.
33 T. A. Taton, C. A. Mirkin and R. L. Letsinger, *Science*, 2000, **289**, 1757.
34 H. Cai, Y. Wang, P. He and Y. Fang, *Anal. Chim. Acta*, 2002, **469**, 165.
35 P. Fanjul-Bolado, D. Hernandez-Santos, M. B. Gonzalez-Garcıa and A. n. Costa-Garcıa, *Anal. Chem.*, 2007, **79**, 5272.
36 M. J. Wang, C. Y. Sun, L. Y. Wang, X. H. Ji, Y. B. Bai, T. J. Li and J. H. Li, *J. Pharm. Biomed. Anal.*, 2003, **33**, 1117.
37 M. Pumera, *Chem. Soc. Rev.*, 2010, **39**, 4146.
38 C. N. R. Rao, A. K. Sood, K. S. Subrahmanyam and A. Govindaraj, *Angew. Chem., Int. Ed.*, 2009, **48**, 7752.
39 Y. Huang, T. H. Wang, J. H. Jiang, G. L. Shen and R. Q. Yu, *Clin. Chem.*, 2009, **55**, 964.
40 E. Braun, Y. Eichen, U. Sivan and G. Ben-Yoseph, *Nature*, 1998, **391**, 775.
41 L. Zhou, L. J. Ou, X. Chu, G. L. Shen and R. Q. Yu, *Anal. Chem.*, 2007, **79**, 7492.
42 K. Z. Brainina, *Talanta*, 1971, **18**, 513.